Down-regulation of the mitochondrial aspartate-glutamate carrier isoform 1 AGC1 inhibits proliferation and N-acetylaspartate synthesis in Neuro2A cells

Emanuela Profilo [a,1], Luis Emiliano Peña-Altamira [b,1], Mariangela Corricelli [c,1], Alessandra Castegna [a], Alberto Danese [c], Gennaro Agrimi [a], Sabrina Petralla [b], Giulia Giannuzzi [a], Vito Porcelli [a], Luigi Sbano [c], Carlo Viscomi [d,e], Francesca Massenzio [b], Erika Mariana Palmieri [a], Carlotta Giorgi [c], Giuseppe Fiermonte [a], Marco Virgili [b], Luigi Palmieri [a,f], Massimo Zeviani [d,e], Paolo Pinton [c], Barbara Monti [b], Ferdinando Palmieri [a,f,*], Francesco Massimo Lasorsa [f,**]

[a] Department of Biosciences, Biotechnologies and Biopharmaceutics, University of Bari 'Aldo Moro', Bari 70125, Italy
[b] Department of Pharmacy and BioTechnology, University of Bologna, Bologna 40126, Italy
[c] Department of Morphology, Surgery and Experimental Medicine, Section of Pathology, Oncology and Experimental Biology, Laboratory for Technologies of Advanced Therapies (LTTA), University of Ferrara, Ferrara 44121, Italy
[d] MRC-Mitochondrial Biology Unit, Cambridge, UK
[e] Fondazione IRCCS Istituto Neurologico "C. Besta", Milan, Italy
[f] Institute of Biomembranes and Bioenergetics, Consiglio Nazionale delle Ricerche, Bari 70126, Italy

ARTICLE INFO

ABSTRACT

The mitochondrial aspartate-glutamate carrier isoform 1 (AGC1) catalyzes a Ca^{2+}-stimulated export of aspartate to the cytosol in exchange for glutamate, and is a key component of the malate-aspartate shuttle which transfers NADH reducing equivalents from the cytosol to mitochondria. By sustaining the complete glucose oxidation, AGC1 is thought to be important in providing energy for cells, in particular in the CNS and muscle where this protein is mainly expressed. Defects in the AGC1 gene cause AGC1 deficiency, an infantile encephalopathy with delayed myelination and reduced brain N-acetylaspartate (NAA) levels, the precursor of myelin synthesis in the CNS. Here, we show that undifferentiated Neuro2A cells with down-regulated AGC1 display a significant proliferation deficit associated with reduced mitochondrial respiration, and are unable to synthesize NAA properly. In the presence of high glutamine oxidation, cells with reduced AGC1 restore cell proliferation, although oxidative stress increases and NAA synthesis deficit persists. Our data suggest that the cellular energetic deficit due to AGC1 impairment is associated with inappropriate aspartate levels to support neuronal proliferation when glutamine is not used as metabolic substrate, and we propose that delayed myelination in AGC1 deficiency patients could be attributable, at least in part, to neuronal loss combined with lack of NAA synthesis occurring during the nervous system development.

© 2017 Elsevier B.V. All rights reserved.

1. Introduction

The mitochondrial aspartate-glutamate carrier (AGC) catalyzes the unidirectional export of mitochondrial aspartate in exchange with cytosolic glutamate plus a proton across the inner mitochondrial membrane [1]. Stimulated by cytosolic calcium [1,2], AGC is a fundamental component of the malate-aspartate shuttle (MAS) which is the main biochemical pathway to transfer NADH reducing equivalents from the cytosol to mitochondria along with the glycerol-3-phosphate shuttle. These processes occur in the various cell types with different efficiency and are indispensable for the complete aerobic oxidation of glucose, preserving the cellular redox state with higher energy yield and efficient ATP production. In humans, AGC exists as two isoforms, AGC1 and AGC2 encoded by *SLC25A12* and *SLC25A13* genes, respectively [1]. Both isoforms share very similar substrate specificity and affinities, although AGC2 show higher transport rates than AGC1 [1]. Mutations in AGC1 and AGC2 are associated with two human diseases [3]. AGC1 deficiency is a severe infantile-onset encephalopathy with epilepsy, global developmental delay, abnormal myelination, and reduced cerebral

* Correspondence to: F. Palmieri, Department of Biosciences, Biotechnologies and Biopharmaceutics, University of Bari 'Aldo Moro', via Orabona, 4, 70125, Italy.
** Correspondence to: F. M. Lasorsa, Institute of Biomembranes and Bioenergetics, Consiglio Nazionale delle Ricerche, via Amendola 165/A, Bari 70126, Italy.
E-mail addresses: ferdinando.palmieri@uniba.it (F. Palmieri), fm.lasorsa@ibbe.cnr.it (F.M. Lasorsa).
[1] These authors contributed equally to this work.

N-acetylaspartate (NAA) content [4,5]. Defects in AGC2 cause adult-onset type 2 citrullinemia [6]. The two disorders have very different clinical pictures related to the higher expression of AGC1 and AGC2 in brain and liver, respectively [7], and are both associated with impaired MAS activity [4,8]. However, biochemical hallmarks of these pathologies appeared not merely linked to a bioenergetic deficit. In type 2 citrullinemia, the loss of aspartate efflux from mitochondria due to AGC2 transport defects induces a liver-specific impairment of argininosuccinate synthetase, a cytosolic enzyme of the urea cycle [6]. Furthermore, hypomyelination in AGC1 deficiency could be secondary to reduced levels of neuronal-generated NAA [5], a precursor for myelin synthesis produced from aspartate and acetyl-CoA by the enzyme aspartate-N-acetyltransferase [9]. Should this evidence demonstrate the physiological role of AGC, AGC isoforms (AGCs) might potentially act as crucial means to supply aspartate from mitochondria for biosynthetic purposes, with respect of the specific function of the cells where the two isoforms are expressed. However, a detailed description of the relative contribution of AGCs in the various tissues is still elusive. This is particularly true in the brain where a controversial expression pattern of AGCs has been hitherto depicted: AGC1 is generally thought to be the main isoform in neurons [10–11], where AGC2 is likewise expressed, although only in restricted brain areas and at low levels [12]. In glial cells, conflicting results did not clarify the expression profile of AGCs in astrocytes [13–16], whereas both isoforms have been reported to be expressed in oligodendrocytes and oligodendrocyte progenitors [17]. The clinical manifestations in AGC1 deficiency suggest that AGC1 should have a predominant role at least in discrete brain cells most likely during brain development.

In the present study, AGC1 was identified as the sole AGC isoform in proliferating mouse neuroblastoma Neuro2A (N2A) cells, while AGC2 is present only during differentiation. Consistently with the importance of AGC in MAS, we showed that AGC1 down-regulation is detrimental to the survival of undifferentiated N2A cells when exclusively fed with substrates producing NADH in the cytosol. By contrast, addition of glutamine rescued the proliferation of N2A cells with reduced AGC1: in these cells, we demonstrated increased glutamine oxidation accompanied by higher mitochondrial ROS production, strongly suggesting the activation of adaptive mechanisms which might favor the generation of substrates supporting proliferation, such as aspartate [18], otherwise impeded by AGC1 inactivation. Furthermore, we demonstrated that NAA levels in undifferentiated N2A neuroblastoma cells are strongly reduced if AGC1 is down-regulated, a defect that can be ascribed not only to insufficient aspartate, but also to the limited pyruvate oxidation subsequent to MAS impairment which prevents the formation of appropriate acetyl-CoA levels for NAA synthesis.

2. Materials and methods

2.1. Cell culture and reagents

Neuro2A cells were purchased from ATCC-LGC Standards (Italy) and cultured at 37 °C in a humidified atmosphere with 5% CO_2 in high glucose DMEM (D6546 SIGMA - Italy) supplemented with 10% fetal bovine serum, 50 U of penicillin G/ml and 50 μg of streptomycin sulfate. In this study, cells were used between #3 and #20 passages. Unless otherwise indicated, cell incubations in minimal growth medium were accomplished by using Minimal Essential Medium (MEM, M5650 SIGMA - Italy). Cell counting was performed using the Scepter™ Automated Cell Counter (Merck Millipore, Germany) according to the manufacturer's instructions, in parallel to trypan blue visualization to exclude significant differences in live/dead trypsinized cells ratio among the tested cells.

2.2. AGC1-silencing shRNA design and lentiviral construct generation for stable transduction of N2A cells.

Two shRNA cassettes 5′-TGCTTGTTCGAAAGATCTATAGCTCGAGC TATAGATCTTTCGAACAAGCTTTTT-3′ and 5′-TGCTTGCAGACCTATATAA

TGCCTCGAGGCATTATATAGGTCTGCAAGCTTTTT-3′ were designed as a hairpin-loop structure from the mouse Slc25a12 cDNA sequence encoding AGC1 protein according to the guidelines described in http://sirna.wi.mit.edu/ [19] and AgeI/EcoRI cloned into the pLKO.1 vector (Sigma - Italy), as previously described [20]. In parallel, a mismatch shRNA 5′-TACAACCAACGCACGCTAATCTCGAGATTAGCGTGCGTTGGT TGTTTTTT-3′ was cloned into the same vector to generate unsilencing control plasmid. The resulting constructs were sequenced and used to transfect HEK293T cells with the Lentiviral Packaging mix (SIGMA - Italy) according to the manufacturer's instructions for the recombinant generation of control LVshMM, and AGC1-silencing LVshAGC1.1 and LVshAGC1.2 lentiviral particles. 4 days after transfection, cell conditioned media containing the virus were harvested, their titer estimated and used for the transduction. N2A cells were transduced with the recombinant LVshMM and LVshAGC1 particles at a viral titer of ~5 plaque-forming units/ml for 24 h at 37 °C and treated with 1 μg/ml puromycin for stable selection.

2.3. Immunoblotting

Total cell extracts or mitochondrion-enriched fractions obtained with Potter-Elvehjem homogenization and serial centrifugations were lysed in RIPA buffer, solubilized in the presence of 10 mM Tris/HCl pH 6.8, 2% SDS, 5% β-mercaptoethanol and subjected to 15% SDS-polyacrylamide gel for subsequent western blot analysis. AGC1, AGC2, UCP2, α-actin and NFL antibodies were purchased from Santa Cruz Biotechnology, Inc. (Dallas, TX USA). AAC antibody was purchased from Mitoscience (Eugene, OR USA). Caspase 3 and PARP-1 antibodies were purchased from Cell Signaling Technology (Danvers, MA USA). Homemade antibodies raised in rabbit against mitochondrial carriers for dicarboxylates (DIC), citrate (CIC), glutamate (GC), phosphate (PiC) and 2-oxoglutarate/malate (OGC) were used. Densitometric analyses were accomplished by using the Image Lab™ Touch software (Bio-Rad Laboratories, CA USA).

2.4. Mitochondrial carriers transport activity measurements

30 μg of isolated mitochondria from N2A cells were solubilized (0.5 mg/ml) in a buffer containing 3% TX-114, 1 mM EDTA, 10 mM PIPES, pH 7.0 for 45 min on ice, and reconstituted in liposomes, as previously described [21]. Transport measurements at 25 °C were initiated by adding radioactive substrates at the indicated concentrations to liposomes reconstituted with mitochondrial extracts containing 20 mM unlabeled substrates and terminated by adding 10 mM pyridoxal 5′-phosphate and 8 mM bathophenanthroline, according to the inhibitor-stop method [1,22]. The incorporated radioactivity was quantified by a LS 6500 liquid scintilation counter (Beckman Coulter, CA USA).

2.5. Measurements of oxygen consumption (OCR) and extracellular acidification rates (ECAR)

OCR and ECAR were simultaneously measured with XF^{96} Extracellular Flux analyzer (Seahorse Bioscience, MA USA). Respiration parameters were also determined through the high resolution O2k respirometer (OROBOROS Instruments, Austria). In Seahorse experiments, 25.000 cells/well were washed three times with unbuffered XF base medium (Seahorse Bioscience, MA USA) without added substrates and then incubated for 1 h in humidified incubator at 37 °C in the presence of unbuffered XF base medium supplemented with 1 g/l glucose + 1 mM pyruvate or 5 mM lactate ± 2 mM glutamine. After incubation, basal OCR/ECAR were recorded three times for total 12 min prior to the sequential injections of 2 μM oligomycin, as inhibitor of ATP synthase (three measurements for total 25 min), 0.2 μM FCCP, as mitochondrial uncoupler (three measurements for total 25 min), and 1 μM antimycin A + 1 μM rotenone, as mitochondrial respiratory chain inhibitors (three measurements for total 25 min). In O2k oxygraphy experiments, 1×10

[6] cells were trypsinized and the cell suspension, treated for 1 h in the same incubation media used for Seahorse experiments, was subsequently subjected to sequential addition of the above mentioned reagents. OCR were measured as previously described [23–25].

2.6. Aequorin and luciferase luminescence measurements

N2A cells were transiently transfected with plasmids carrying the coding sequence of recombinant aequorins selectively targeted to the cytosol (cytAEQ) or mitochondria (mtAEQmut), and of the recombinant luciferase targeted to mitochondria (mtLuc) [2]. Transfected cells were incubated for 1 h at 37 °C with KRB supplemented with 1 mM CaCl$_2$, 1 g/l glucose, 1 mM pyruvate and 2 mM glutamine (+5 μM coelenterazine for aequorins reconstitution). Cells were subsequently perfused in the same buffer (+20 mM luciferin for luciferase assays) in a purpose-built luminometer where they were stimulated with 1 mM ATP. Aequorin experiments were terminated by lysing the cells in a hypotonic solution with 0.1 mM digitonin and 10 mM CaCl$_2$, and light output was collected and calibrated in [Ca^{2+}], as previously described [26]. In luciferase assays, data are expressed as mtLuc light output percentage of cells before agonist stimulus.

2.7. Cell fluorescence analysis

Measurements of intracellular reactive oxygen species were performed by loading cells with 5 μM 5-(and-6)-chloromethyl-2′,7′-dichlorodihydrofluorescein diacetate, acetyl ester (CM-H2DCFDA; Life Technologies, C-6827) for 20 min at 37 °C, and green fluorescence of cells was analyzed with a Tali® Image-Based Cytometer. Mitochondrial hydrogen peroxide levels were measured in N2A cells cultured on 24 mm glass coverslips and transfected with the ratiometric fluorescent probe with mitochondrial localization pHyPer-dMito (mt-HyPer) [27]. After 24 h expression, cells were maintained in KRB supplemented with 1 mM CaCl$_2$ and the indicated carbon sources, and placed in an open Leyden chamber on a 37 °C thermostated stage. 494/406 nm excitation filters and a 500-nm long-pass beam splitter were used, and an image pair was obtained in every 200 ms with a ×40 objective. For a ratiometric measurement, at the end of each measurement, the efficiency of the probe was ascertained by adding H$_2$O$_2$ as reference. Fluorescence data were expressed as emission ratios. The experiments were performed on a Cell^R Olympus multiple wavelength high-resolution epi-fluorescence microscope. Mitochondrial inner membrane potential (Ψm) was measured by loading the cells with 20 nM tetramethyl rhodamine methyl ester (TMRM; Life Technologies, T-668) for 30 min at 37 °C. Images were taken on an inverted Nikon LiveScan Swept Field Confocal Microscope (*SFC*) Eclipse Ti equipped with NIS-Elements microscope imaging software (Nikon Instruments). TMRM fluorescence intensities (exc. 560 nm; emis. 590–650 nm) were imaged every 5 s with a fixed 20 ms exposure time. At the end of the experiments, 10 μM FCCP was added after 240 acquisitions to completely collapse the Ψm and to subtract the non-mitochondrial TMRM fluorescence, as previously described [28].

2.8. Metabolite determinations by mass spectrometry

For metabolite quantification, LVshMM-N2A and LVshAGC1-N2A cells were starved for 1 h in KRB without carbon sources and subsequently incubated in Minimum Essential Medium Eagle (MEM) (Sigma M5650) supplemented with 1 g/l glucose, 5 mM lactate, and with or without 2 mM glutamine. After the indicated incubation times, conditioned MEM and cells were harvested, extracted with methanol/water (50–50), and the aqueous phase was centrifuged at 13,000 *g* for 20 min at 4 °C to precipitate the protein fraction. A Quattro Premier mass spectrometer with an Acquity UPLC system (Waters - Italy) was used for electrospray ionization LC-MS/MS analysis in the multiple reaction monitoring (RMR) mode, as previously described [20]. The MRM

transitions in the negative-ion mode were *m/z* 190.95 > 110.89 for citrate, *m/z* 116.88 > 73.20 for succinate, *m/z* 115.07 > 71.31 for fumarate, *m/z* 132.95 > 115.20 for malate, *m/z* 144.9 > 101.10 for 2-oxoglutarate, and *m/z* 174.1 > 88.0 for NAA. The MRM transitions in the positive-ion mode were *m/z* 134.16 > 73.76 for aspartate, *m/z* 148.20 > 83.80 for glutamate, *m/z* 90.00 > 44.24 for alanine, and *m/z* 308.28 > 179.02 for reduced glutathione. Calibration curves of standards were used for metabolites quantifications.

2.9. Respiratory chain complex analysis

Mitochondrial respiratory chain complex and citrate synthase activities were measured in permeabilized cells using a Cary 50 spectrophotometer (Agilent Technologies Santa Clara, CA USA), as previously described [29] with some modification. The NADH-ubiquinone oxidoreductase activity of complex I was measured quantifying the decrease in UV absorbance accompanying the oxidation of NADH. Any rotenone-insensitive activity was measured. Succinate dehydrogenase/complex II activity was measured following the reduction of 2.6-dichlorophenolindophenol (DCPIP) at 600 nm after the addition of succinate. Complex II + III (succinate cytochrome *c* reductase) activity was measured following the reduction of oxidized cytochrome *c* at 550 nm coupled to succinate oxidation. The activity of complex IV was carried out by evaluating the oxidation of reduced cytochrome *c* at 550 nm. ATPase activity was measured at 340 nm by coupling the production of ADP to the oxidation of NADH via pyruvate Kinase and lactate dehydrogenase. The reactions were measured for 2 min under controlled temperature, with a linear slope in the presence or absence of inhibitor when present, and enzymatic activity of each complex was normalized to that of citrate synthase.

3. Results

3.1. AGC1 is the only isoform of the mitochondrial aspartate/glutamate carrier expressed in undifferentiated N2A cells

The impact of AGC1 on neuron function was investigated in mouse brain-derived N2A cells previously reported as a reliable model to evaluate neuron proliferation, metabolism and differentiation [30–32]. In agreement with Ramos and coworkers [13], WB analysis (Fig. 1A) performed with N2A cells revealed the increasing expression of AGC1 after differentiation with dibutiryl-AMPc. AGC2 isoform was instead detected at constant levels only after cell differentiation, thus suggesting that in undifferentiated proliferating N2A cells MAS works uniquely in the presence of AGC1. Therefore, we stably down-regulated AGC1 expression in N2A cells by using two lentiviral constructs (LVshAGC1-N2A.1 and LVshAGC1-N2A.2) that individually allowed a ~75% reduction of AGC1 protein even after cell differentiation and without affecting AGC2 expression, as compared to N2A cells stably transduced with a lentiviral control construct (LVshMM-N2A) (Fig. 1B). It should be noted that, due to space limit, in Fig. 1B, as well as in all other reported results, only data referred to LVshAGC1-N2A.1 silenced cells are shown, unless otherwise indicated, and similar results were also obtained with LVshAGC1-N2A.2 silenced cells. As measured with mitochondrial extracts reconstituted in liposomes (Fig. 1C), AGC1 silencing in undifferentiated LVshAGC1-N2A cells reduced both the aspartate/glutamate and the glutamate/glutamate exchange activities by ~80% and ~50%, respectively, when compared to those measured with mitochondria isolated from control cells. On one side, these data demonstrated the efficiency of silencing to knock down AGC1 activity, while on the other hand they suggested the presence in N2A cells of alternative mitochondrial proteins able to perform glutamate transport, such as the mitochondrial glutamate carrier (GC) isoforms [33] (see below). It is noteworthy that AGC1 activity in LVshAGC1-N2A cells is basically similar to that revealed in patients with AGC1 function dramatically reduced, but not totally abolished [5].
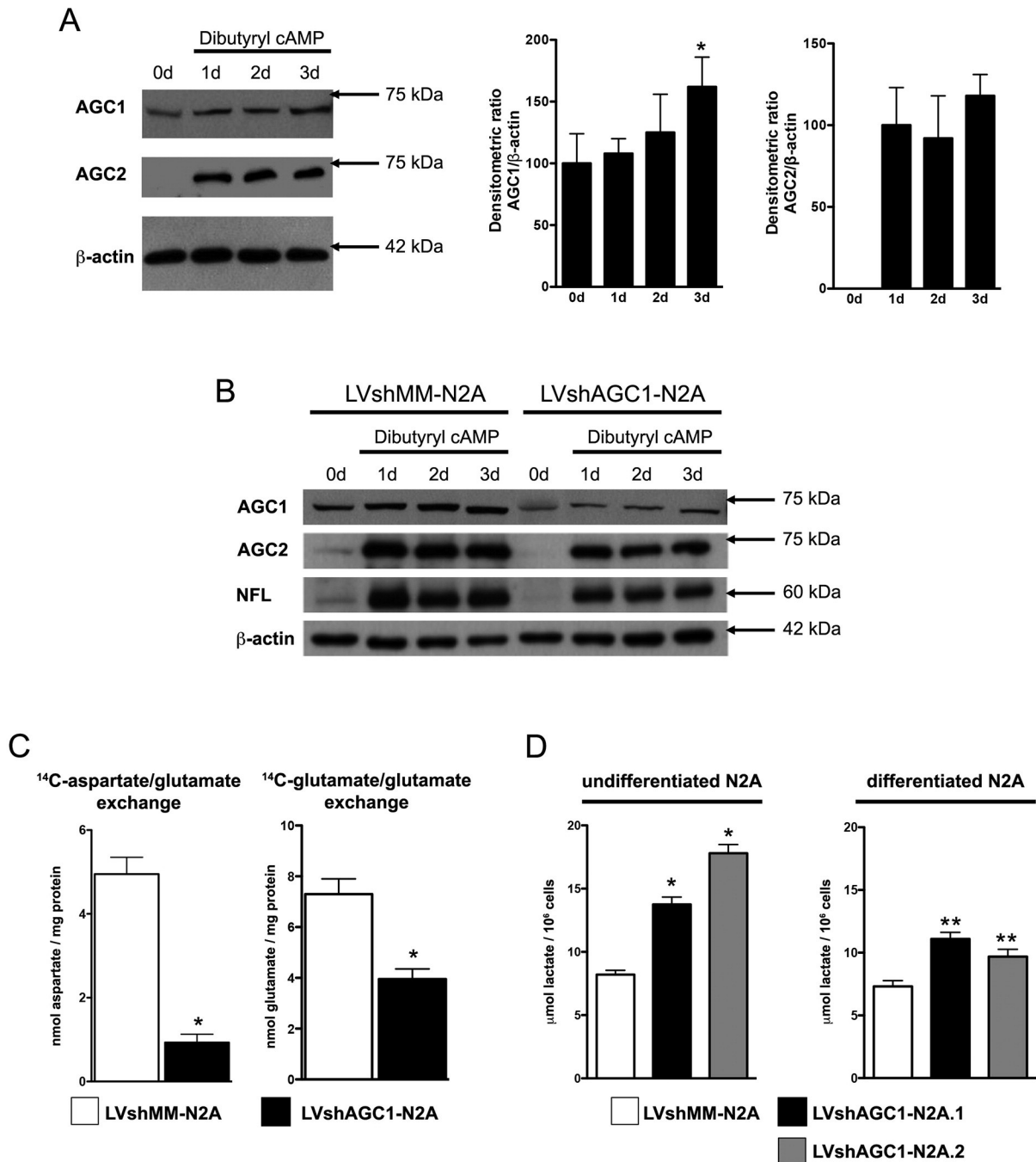
Fig. 1. Down-regulation of AGC1 increases lactate release in conditioned medium of N2A cells. (A) N2A cells were treated with 1 mM dibutyryl-cAMP, as differentiating agent, and harvested every 24 h for western blot analysis. 30 ∝g of cell lysate were used to react with antisera raised against the indicated proteins. Histogram graphs show the means ± SD of the densitometric ratios between either AGC1 or AGC2 and β-actin from three independent experiments. *$p < 0.05$ vs undifferentiated cells. (B) N2A cells stably transduced with either control LVshMM or LVshAGC1 construct were differentiated with 1 mM dibutyryl-cAMP and harvested every 24 h for western blot analysis. 30 ∝g of cell lysate were used to react with antisera raised against the indicated proteins. The neurofilament light chain protein (NFL) was monitored to evaluate neuronal maturation. (C) Aspartate/glutamate and glutamate/glutamate exchange activities were assayed in liposomes reconstituted with mitochondrial extracts from undifferentiated N2A cells stably transduced with control LVshMM (white bars) or LVshAGC1 (black bars) construct. Transport was initiated by adding 50 μM [^{14}C]aspartate (left panel) or 0.2 mM [^{14}C]glutamate (right panel) to reconstituted liposomes both preloaded with 20 mM glutamate. The reaction times were 15 min. Data are means ± SD from 4 independent experiments performed in triplicate. *$p < 0.01$ vs LVshMM-N2A cells, one-way analysis with Bonferroni t-test. (D) Lactic acid was quantified in conditioned complete DMEM harvested from control LVshMM-N2A cells (white bars) or LVshAGC1-N2A.1 and LVshAGC1-N2A.2 cells (black and grey bars). Conditioned media from undifferentiated cells were harvested after 24 h incubation; conditioned media from differentiated cells were harvested 24 h after addition of 1 mM dibutyryl-cAMP. Values are the means ± SD from 3 independent experiments performed in triplicate. *$p < 0.01$; **$p < 0.05$ vs LVshMM-N2A cells; one-way analysis with Bonferroni t-test.

The effect of reduced AGC1 activity on the transfer of the NADH reducing equivalents from the cytosol to mitochondria was then tested by measuring lactic acid secreted by N2A cells grown in complete DMEM (Fig. 1D). As expected, after 24 h incubation the lactic acid released in the conditioned DMEM harvested from undifferentiated LVshAGC1-N2A cells was from 70% to 120% higher than that of control cells, while in media from differentiated LVshAGC1-N2A cells, lactic acid was ~40% more than in medium from differentiated LVshMM-N2A cells (Fig. 1D). Since the down-regulation of AGC1 inhibits MAS activity, these data suggested that LVshAGC1-N2A cells consume glucose

preferentially in the cytosol, thus increasing the production of lactate from glycolysis-derived pyruvate, which regenerates NAD$^+$. Furthermore, the contemporary expression of AGC2 may only partially compensate the AGC1 deficit after cell differentiation.

3.2. Down-regulation of AGC1 inhibits proliferation and mitochondrial respiration of N2A cells

Given that no difference in the proliferation of LVshAGC1-N2A and LVshMM-N2A cells cultured in complete rich DMEM was observed (data not shown), an altered glucose metabolism in AGC1-silenced cells suggested that LVshAGC1-N2A growth was sustained by alternative utilization of other metabolites. Therefore, N2A cells were cultured for several days in minimal growth media (MEM) containing glucose in combination with other substrates for neurons, such as lactate or pyruvate in the presence or absence of glutamine [34] (Fig. 2A). LVshAGC1-N2A and control LVshMM-N2A cell number was not significantly different when grown in the presence of glucose with either pyruvate or lactate supplemented with glutamine, with the exception of the first measurements at 24 h and 48 h. Interestingly, when MEM was deprived of glutamine, LVshAGC1-N2A cells failed to proliferate at the same rate of control cells. In particular, in the presence of glucose and pyruvate LVshAGC1-N2A cell number was markedly lower than that

of LVshMM-N2A cells, while in the presence of glucose and lactate LVshAGC1-N2A cells started to die after 24–36 h of incubation. It should be also noted that N2A cells were unable to grow in MEM when only glucose was added (data not shown). As shown in Fig. 3A and B, the measurements of cell respiration parameters in the presence of the above mentioned substrates revealed a diminished respiratory capacity of N2A cells with impaired AGC1 activity in the absence of glutamine. More in the detail, the basal (routine) respiration of LVshAGC1-N2A cells incubated for 1 h with minimal medium supplemented with glucose plus either pyruvate or lactate was ~25% and ~45% decreased, respectively, when compared to control LVshMM-N2A cells, as in part previously described for intact cortical neurons with deficient AGC1 [10]. On the other hand, no difference in basal respiration of both cell types was found when glutamine was added to the medium (Fig. 3A and B). Moreover, the absence of glutamine in the incubation medium caused a significant decrease in both mitochondrial Electron Transfer System (ETS) capacity, i.e., maximal respiration with FCCP, and ATP turnover of LVshAGC1-N2A cells (Fig. 3A and B). To verify whether bioenergetic deficits and the reduced proliferation of LVshAGC1-N2A cells could be associated with higher cell mortality, in the same experimental conditions we estimated the cleavage of PARP1 and Caspase 3 proteins (Fig. 2B), as markers of an occurring apoptotic process [35,36]. After 1 h incubation in MEM supplemented with glucose and either pyruvate
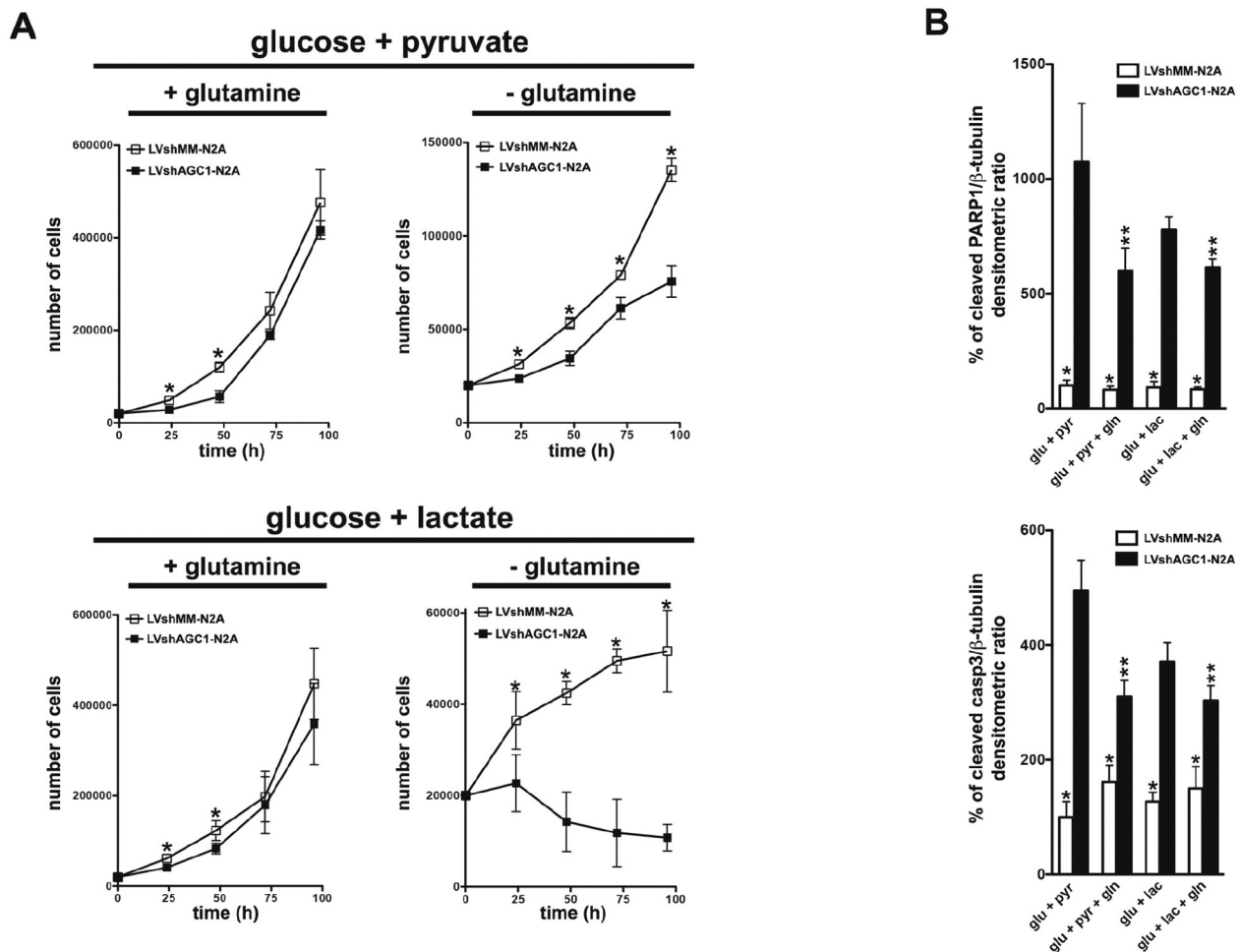
Fig. 2. Glutamine deprivation reduces proliferation of N2A cells with down-regulated AGC1. (A) Cell count for LVshMM-N2A (white squares) and LVshAGC1-N2A (black squares) cells grown in MEM supplemented with 1 g/l glucose + 1 mM pyruvate or 5 mM lactate ± 2 mM glutamine. Cells were detached at the indicated times and counted using the Scepter™ Automated Cell Counter (Merck Millipore, Germany). Data are means ± SD from five independent time courses. *p < 0.001 compared to control LVshMM-N2A cells at the corresponding time point; one-way analysis with Bonferroni t-test. (B) Relative quantitative analysis of apoptotic markers in LVshMM-N2A cells (white columns) and LVshAGC1-N2A (black columns) incubated 1 h in MEM supplemented with 1 g/l glucose + 1 mM pyruvate or 5 mM lactate ± 2 mM glutamine. Data are means ± SD of relative densities of 89 kDa cleaved PARP1 (upper panel) and 17 kDa cleaved caspase-3 (lower panel) proteins versus β-tubulin from 3 independent western blots. *p < 0.01 compared to LVshAGC1-N2A cells incubated with the same medium; **p < 0.05 compared to LVshAGC1-N2A cells incubated with the same medium without glutamine; one-way analysis with Bonferroni t-test.
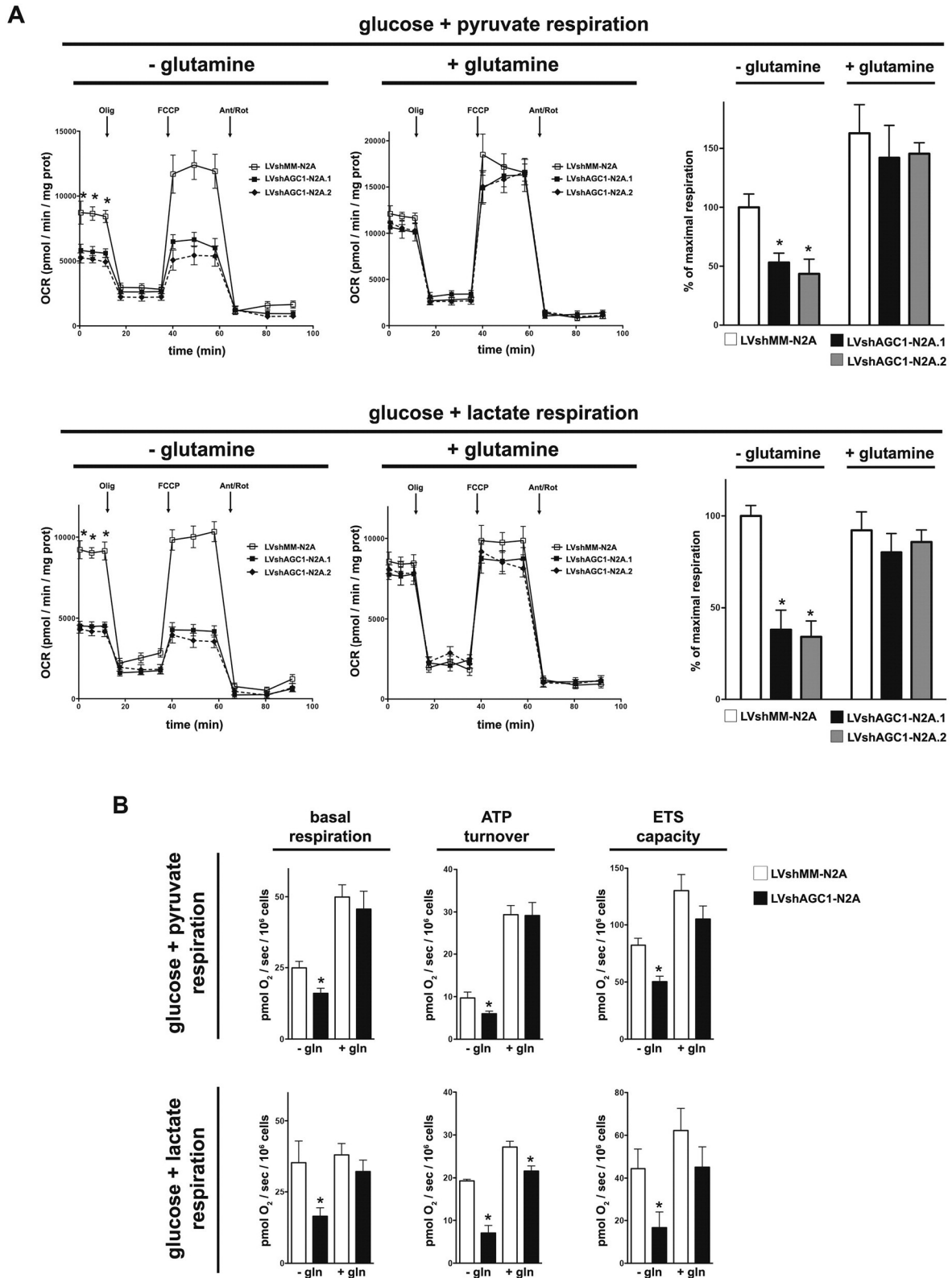
Fig. 3. Glutamine deprivation inhibits mitochondrial respiration in N2A cells with down-regulated AGC1. Oxygen consumption rates (OCR) were measured with XF[96] extracellular flux analyzer (SeaHorse) (A) and O2k oxygraph (Oroboros) (B) in LVshMM-N2A and LVshAGC1-N2A cells incubated for 1 h in base medium supplemented with 1 g/l glucose + 1 mM pyruvate or 5 mM lactate ± 2 mM glutamine. N2A cells were exposed to sequential additions of 2 μM oligomycin, 0.2 μM FCCP, and 1 μM antimycin A + 1 μM rotenone. In Seahorse experiments, OCR data are mean values ± SD from three independent experiments each including 5–6 replicates per cell type; *$p < 0.01$ compared to LVshAGC1-N2A.1 and LVshAGC1-N2A.2 cells at the corresponding time point; one-way analysis with Bonferroni t-test; maximal respiration data with FCCP have been expressed as percentage of values compared with those of LVshMM-N2A cells incubated in the absence of glutamine, *$p < 0.01$. In O2k oxygraph measurements, data are means ± SD from three independent experiments performed in duplicates; *$p < 0.01$ as compared to LVshMM-N2A cells incubated with the same medium.

or lactate, LVshAGC1-N2A cells displayed a dramatic increase of both apoptotic markers, as compared to control LVshMM-N2A cells. Notably, in the presence of glutamine, the apoptosis in LVshAGC1-N2A cells, while still enhanced, was significantly reduced. All together these data suggested a role of glutamine to sustain mitochondrial respiration and cell viability in undifferentiated N2A cell when AGC1 levels are impaired.

3.3. Down-regulation of AGC1 alters mitochondrial Ca^{2+} homeostasis in N2A cells

AGCs are Ca^{2+}-stimulated carriers that allow higher mitochondrial pyruvate oxidation when $[Ca^{2+}]$ increases in the cytosol [10]. Therefore, we simultaneously measured the extracellular acidification rate (ECAR) and OCR of N2A cells challenged by ATP that elicits IP₃-mediated

mobilization of Ca^{2+} from intracellular stores [37]. ECAR significantly decreased in stimulated LVshMM-N2A cells when compared to that of LVshAGC1-N2A cells independently whether either glucose and pyruvate (Fig. 4A) or glucose and lactate (not shown) ± glutamine were used as incubation substrates. Surprisingly, in the same experimental conditions, the expected increase of OCR after ATP stimulation was virtually the same in both control and AGC1 silenced N2A cells (Fig. 4B). ECAR data confirmed that in the presence of higher $[Ca^{2+}]_c$, mitochondrial pyruvate consumption underlying cell respiration cannot be boosted when MAS is deficient [10] and suggest that glutamine supply does not modify the mitochondrial Ca^{2+}-stimulated pyruvate metabolism. On the other hand, OCR measurements suggested that in undifferentiated N2A cells with reduced AGC1, additional factors might maintain a high respiration rate when intracellular Ca^{2+} signals are triggered. As measured with Ca^{2+}-sensitive recombinant aequorins
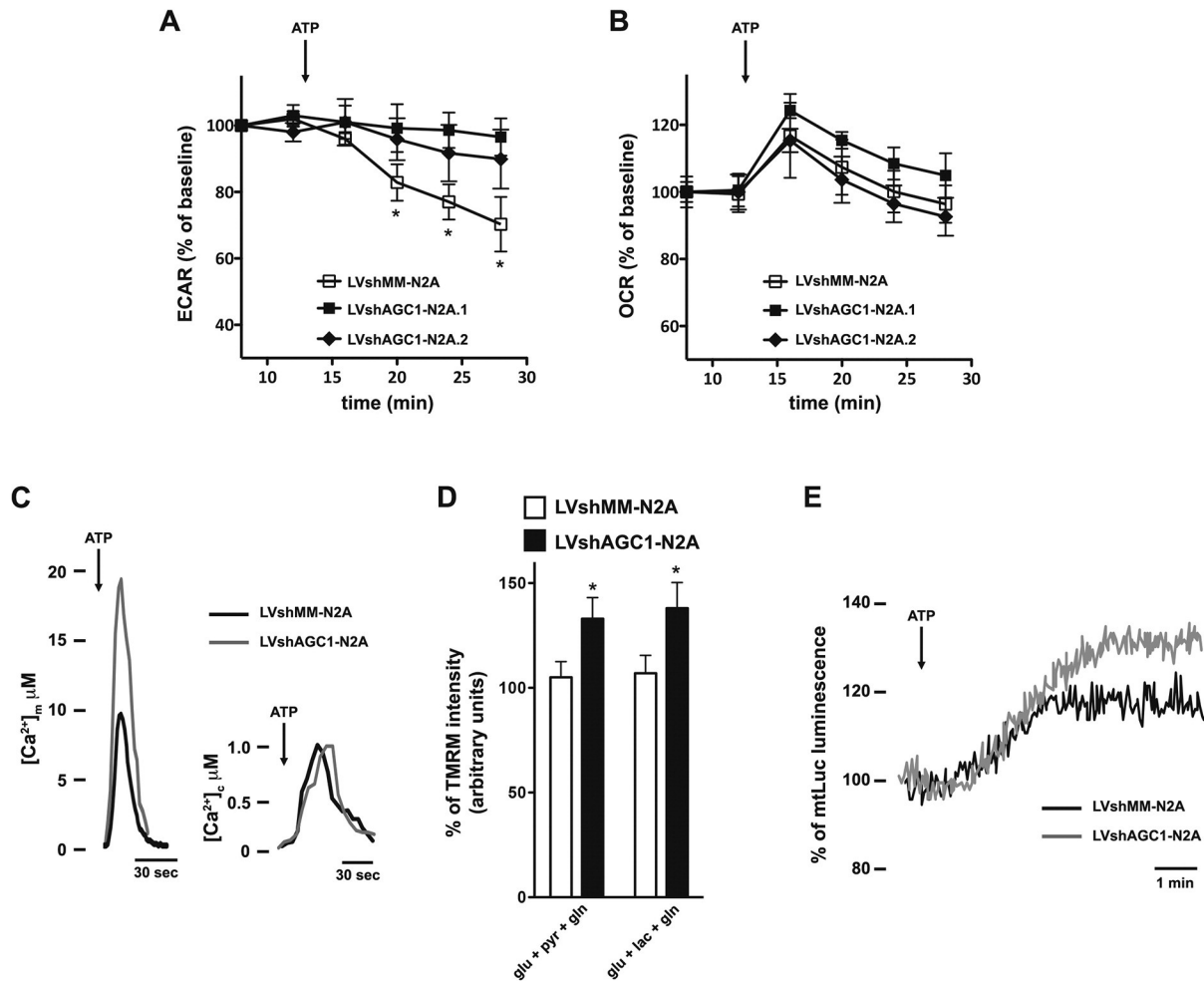
Fig. 4. Enhanced Ca^{2+}-dependent mitochondrial response in stimulated N2A cells with down-regulated AGC1. ECAR (A) and OCR (B) were simultaneously measured with XF⁹⁶ extracellular flux analyzer (SeaHorse) in LVshMM-N2A or LVshAGC1-N2A.1 or LVshAGC1-N2A.2 cells incubated for 1 h in base medium supplemented with 1 g/l glucose + 1 mM pyruvate + 2 mM glutamine and stimulated with 1 mM ATP at the indicated time. ECAR and OCR were normalized to basal values before agonist stimulation and expressed as means ± SD from three independent experiments each including 5–6 replicates per cell type; *$p < 0.05$ compared to two separate LVshAGC1-N2A cell cultures at the corresponding time point; one-way analysis with Bonferroni t-test. (C) $[Ca^{2+}]$ were measured in N2A cells transiently expressing recombinant aequorins targeted to the cytosol (right panel) or mitochondria (left panel) of LVshMM-N2A and LVshAGC1-N2A cells. Cells were perfused with Krebs-Ringer buffer (KRB: 135 mM NaCl, 5 mM KCl, 1 mM MgSO₄, 0.4 mM KH₂PO₄, 20 mM HEPES, pH 7.4) supplemented with 1 mM CaCl₂, 1 g/l glucose, 1 mM pyruvate and 2 mM glutamine, and challenged with 1 mM ATP. Shown traces are representative of the following measurements: for LVshMM-N2A cells, $[Ca^{2+}]_c$ peak values, 1.01 ± 0.11 μM, $n = 20$; $[Ca^{2+}]_m$ peak values, 9.51 ± 2.41 μM, $n = 20$; for LVshAGC1-N2A cells, $[Ca^{2+}]_c$ peak values, 1.20 ± 0.15 μM, $n = 20$; $[Ca^{2+}]_m$ peak values, 17.5 ± 3.11 μM, $n = 20$. (D) Relative increases of $\Delta\psi_m$ after Ca^{2+}-releasing agonist stimulation were measured by fluorescence microscopy in LVshMM-N2A and LVshAGC1-N2A cells incubated for 1 h in base medium supplemented with 1 g/l glucose, either 1 mM pyruvate or 5 mM lactate, and 2 mM glutamine. Cells were loaded with 20 nM TMRM for 30 min at 37 °C and fluorescence intensities were imaged every 5 s with a fixed 20 ms exposure time. ATP 100 μM was added after 6 acquisitions to induce the Ca^{2+} release from the intracellular stores. Data are means ± SD of TMRM percentage intensities normalized to values before agonist stimulation in three independent experiments; *$p < 0.001$ compared to LVshMM-N2A cells. (E) ATP-dependent luminescence was measured in LVshMM-N2A and LVshAGC1-N2A cells expressing mtLuc and incubated for 1 h in KRB supplemented with 1 mM CaCl₂, 1 g/l glucose, 1 mM pyruvate and 2 mM glutamine. In the luminometer, cells were perfused in the same medium and challenged with 1 mM ATP. Data are expressed as percentage of mtLuc light output increase from cells normalized to the prestimulatory values. Shown traces are representative of the following results: for LVshMM-N2A cells, 18.1 ± 3%, $n = 20$ of the prestimulatory value; for LVshAGC1-N2A cells: 28.8 ± 5%, $n = 20$.

(Fig. 4C), in both stimulated control and AGC1-silenced N2A cells expressing cytosolic aequorin (cytAEQ), $[Ca^{2+}]_c$ peaks were virtually the same. Instead, LVshAGC1-N2A cells expressing the mitochondrially targeted aequorin (mtAEQmut) showed a two-fold increased mitochondrial Ca^{2+} accumulation as compared to control LVshMM-N2A cells. Remarkably, the higher mitochondrial Ca^{2+} uptake resulted supported by a more elevated mitochondrial membrane potential ($\Delta\psi_m$) in response to the agonist (Fig. 4D), and accompanied by a significant enhancement of the Ca^{2+}-induced mitochondrial ATP synthesis in silenced LVshAGC1-N2A cells (Fig. 4E). All together these results indicated that in cells with down-regulated AGC1 a stronger activation of the mitochondrial Ca^{2+}-dependent pyruvate, isocitrate and 2-oxoglutarate

dehydrogenases may take place [37], thus in turn further stimulating the mitochondrial metabolic machinery.

3.4. Metabolomic analysis of AGC1-silenced N2A cells reveals an increased consumption of TCA cycle intermediates

Taken together, our data suggested that AGC1-silenced N2A cells might adapt their metabolism to stimulate mitochondrial activity, in particular by strengthening both mitochondrial Ca^{2+}-sensitivity and glutamine oxidation. By LC-MS/MS analysis, we studied whether increased glutamine expenditure occurs in N2A cells with down-regulated AGC1. As shown in Fig. 5A and C, the uptake of glutamine in LVshAGC1-N2A
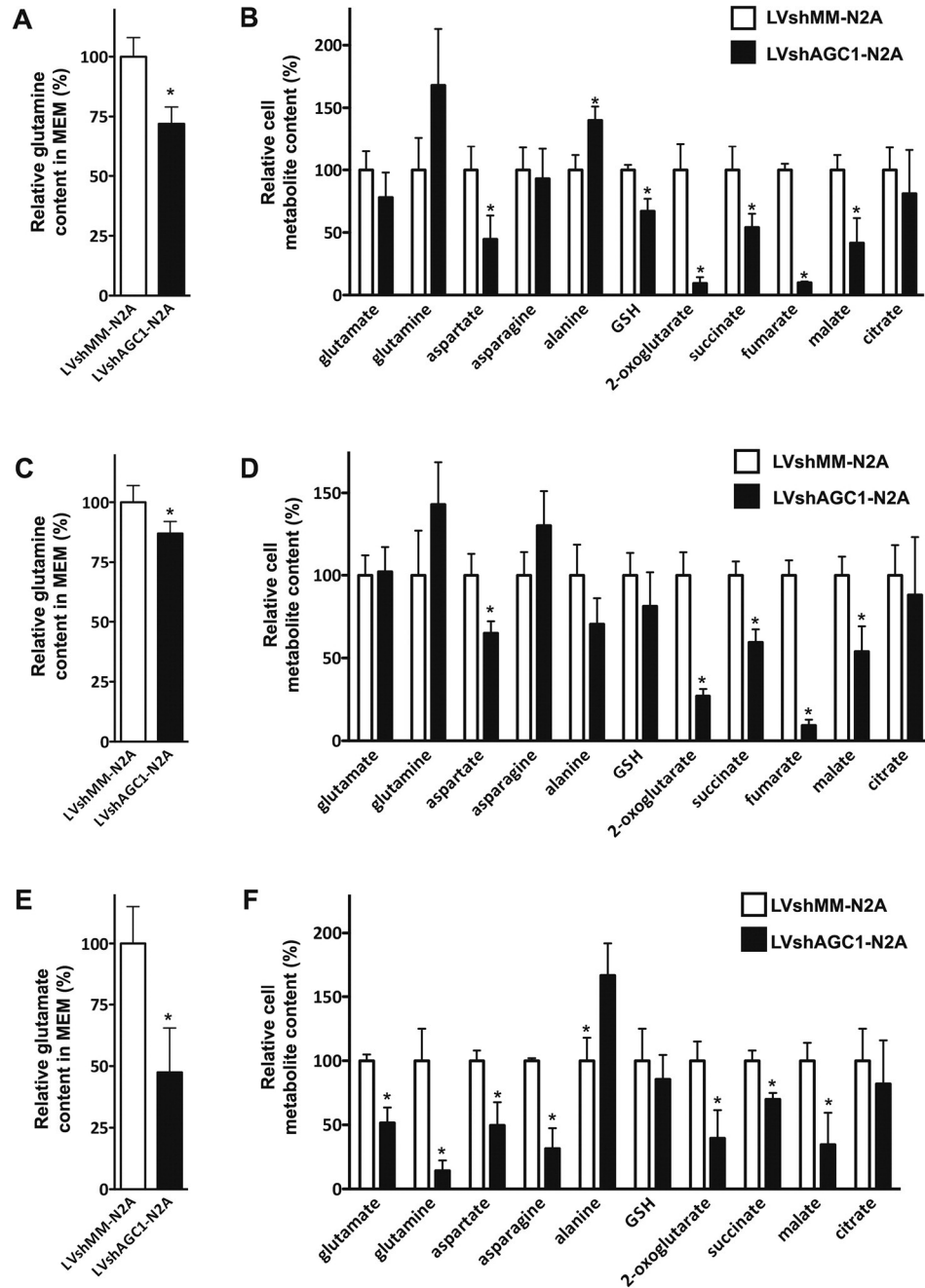
Fig. 5. Relative metabolite content in N2A cells with down-regulated AGC1. Media from LVshMM-N2A and LVshAGC1-N2A cells were harvested after 1 h (A and B) and 6 h (C and D) incubation with MEM supplemented with 1 g/l glucose, 5 mM lactate and 2 mM glutamine. Media and cells were also harvested after 1 h incubation with the same medium deprived of glutamine (E and F). Glutamine (A and C) and glutamate (E) levels in MEM, and the total cell pools of L-glutamate, L-glutamine, L-aspartate, L-asparagine, L-alanine, reduced glutathione, 2-oxoglutarate, succinate, fumarate, L-malate and citrate (B, D and F) were determined by mass spectrometry. Error bars represent the SD of three independent preparations, *$p < 0.05$ compared with LVshMM-N2A cells, one-way analysis with Bonferroni t-test.

cells was markedly increased compared to LVshMM-N2A cells (~ 25% and ~ 15%, after 1 h and 6 h incubation, respectively). Consequently, the relative glutamine content in LVshAGC1-N2A cells was higher than in control cells, although not significantly (Fig. 5B and D). These data indicated that glutamine is not only efficiently imported, but also highly consumed by N2A cells when AGC1 is silenced. Interestingly, when cells were deprived of glutamine (Fig. 5E), LVshAGC1-N2A took ~ 50% more glutamate from the culture medium and the intracellular glutamate content was ~ 50% reduced (Fig. 5F), as compared to control cells. By extending our analysis to other amino acids and TCA cycle intermediates, after 1 h incubation, LVshAGC1-N2A cells showed a significant increase of intracellular alanine which is consistent with reduced mitochondrial pyruvate oxidation [38], and marked decrease of aspartate as well as of 2-oxoglutarate, succinate, fumarate and malate, but not of citrate, as compared to LVshMM-N2A cells (Fig. 5B and F). Similar results were obtained when measurements were performed after 6 h incubation in medium containing glutamine with the only exception for alanine content which appeared restored to values similar to those of control cells (Fig. 5D). Therefore, although in the presence of inhibited pyruvate oxidation, N2A cells with low AGC1 activity appear able to consume at a higher rate the TCA cycle intermediates downstream of glutamate deamination [39].

3.5. Changes in mitochondrial protein activity are associated with higher ROS generation in AGC1-silenced N2A cells

Mass spectrometry data prompted us to investigate the activity of members of the mitochondrial carrier family that may potentially lower or increase the concentration of TCA cycle intermediates in anaplerosis and/or cataplerosis [40]. As shown in Fig. 6A, the expression of mitochondrial carriers CIC, GC, AAC and DIC resulted unvaried in both LVshMM-N2A and LVshAGC1-N2A cells. The mitochondrial UCP2 carrier, a mitochondrial exchanger of aspartate with other C4 metabolites [20], appeared somewhat reduced in LVshAGC1-N2A cells, although not significantly. Most notably, N2A cells with reduced AGC1 revealed a striking increase in both expression and transport activity of the mitochondrial carriers for phosphate (PiC) and 2-oxoglutarate/malate (OGC), the latter participating together with AGC in the MAS [22]. It should be noted that similar changes in mitochondrial carrier expression profile occurred in cells grown with minimal growth medium (data not shown). Furthermore, we investigated whether the mitochondrial respiratory chain was affected by AGC1 silencing. The activity of mitochondrial respiratory chain complexes II, II + III, IV and ATP synthase were not significantly different in both LVshMM-N2A and LVshAGC1-N2A cells. By contrast, a significant decrease in complex I activity in LVshAGC1-N2A cells was found (Fig. 6B). Since increased production of hydroxyl radicals has been ascertained in mitochondrial pathologies with complex I deficiency [41,42] and is a recurrent cause of neuronal loss [43,44], ROS generation in both cytosol and mitochondria of AGC1-silenced N2A cells was measured (Fig. 6C). We detected a more pronounced mitochondrial ROS generation in LVshAGC1-N2A cells compared to control cells grown in complete rich DMEM. To better understand whether ROS production was dependent on substrate supply, mtHyper ratiometric fluorescence was measured in cells incubated in minimal growth medium. When N2A cells were supplemented with glucose plus either pyruvate or lactate, there was no significant difference in the high ROS synthesis between LVshAGC1-N2A and LVshMM-N2A cells. By contrast, the addition of glutamine to the medium significantly mitigated mitochondrial ROS production in control cells, but, importantly, not in LVshAGC1-N2A cells which appeared subjected to higher oxidative stress in each tested condition. As a result, these data suggested a protective role of glutamine against ROS synthesis in mitochondria that lacks in N2A cells with knocked-down AGC1.

All together these data denote that undifferentiated N2A cells with low AGC1 activity may survive only by adapting their metabolism, expending more glutamine with the deleterious consequence of increasing oxidative stress. By interpreting OCR and HPLC/MS data

(Figs. 3A, B and 5), higher glutamine utilization by AGC1-silenced N2A cells would both enforce the Krebs cycle and provide metabolites for biosyntheses and cell proliferation. In our hypothesis (see Fig. 7 and discussion), in the absence of an efficient AGC which provides aspartate in the cytosol, glutamine may represent an alternative source for this amino acid essential in proliferating cells [18,45].

3.6. Impaired AGC1 activity inhibits N-acetylaspartate synthesis in N2A cells

Aspartate along with acetyl-CoA is required for the synthesis of N-acetylaspartate (NAA) by the neuronal aspartate N-acetyltransferase (ANAT) [9,46,47]. NAA is the precursor of myelin lipids in the brain and is severely reduced in patients affected by AGC1 deficiency where AGC1 activity is either absent [4] or significantly inhibited [5]. Indeed, N2A cells with silenced AGC1 revealed a striking deficit of NAA content compared to control cells, which was not rescued even when cells were incubated with glutamine for longer time (6 h) (Fig. 8). These data suggested that aspartate produced in N2A cells with reduced AGC1 might be preferably utilized for proliferation process. However, it could be also argued that AGC1 activity impairment, which in turn inhibits pyruvate oxidation in N2A mitochondria, might generate insufficient levels of acetyl-CoA to participate in ANAT reaction, thus unable to synthesize appropriate NAA levels.

4. Discussion

Recent advances in bioenergetics studies have emphasized a crucial role for mitochondria in the proper development of the nervous system [48,49]. The significant number of neurological pathologies associated with inborn mitochondrial dysfunctions in humans [50,51] further suggests the primary importance of the correct fulfilment of bioenergetic processes in order to sustain healthy brain maturation. Brain energetic metabolism is primarily based on glucose oxidation, and mitochondria emerge as central organelles to allow the metabolic changes underpinning neuronal and glial cells function in the different stages of brain differentiation [52]. In particular, it has been recently demonstrated that improved bioenergetics with increased mitochondrial activity is required when neuronal differentiation takes place [48]. Neurons normally oxidize almost exclusively glucose through the combined activity of glycolysis and TCA cycle for subsequent ATP synthesis [53]. Furthermore, although controversial and highly debated, evidence supports the existence of the astrocyte-neuron lactate shuttle, where the glucose-derived lactate released from astrocytes is taken up and oxidized by neurons as an additional or alternative energy substrate [54–56]. Oxidation of either glucose- or lactate-derived pyruvate in neurons requires the correct transfer of NADH reducing equivalents from the cytosol to mitochondria. Therefore, being the malate/aspartate NADH shuttle the main redox shuttle system in brain [53,57,58], the activity of Ca^{2+}-regulated AGC isoforms becomes crucial for healthy brain functions. However, the relative contribution of AGC1 and AGC2 in the modulation of bioenergetics and mitochondrial metabolism in neurons and other brain cells has not yet been fully elucidated. As an example, several studies have so far depicted a controversial expression pattern of AGC in neurons, where AGC1 is thought to be the main isoform and AGC2 has been shown to be expressed only at low levels in discrete brain regions [12]. In the present study, we have identified in undifferentiated mouse brain-derived N2A cells, a neuronal cell model expressing uniquely AGC1. In our hands, diversely to AGC1, AGC2 is virtually undetectable in proliferating N2A cells, whereas both AGC isoforms are simultaneously expressed when cells are committed to complete differentiation (Fig. 1A). This experimental evidence suggested that AGC1 might have an irreplaceable energetic function during N2A cell proliferation, while AGC2 could be recruited to sustain increased mitochondrial bioenergetics in the subsequent stages of neuronal differentiation. Indeed, when pyruvate or lactate where used with glucose as the sole respiratory
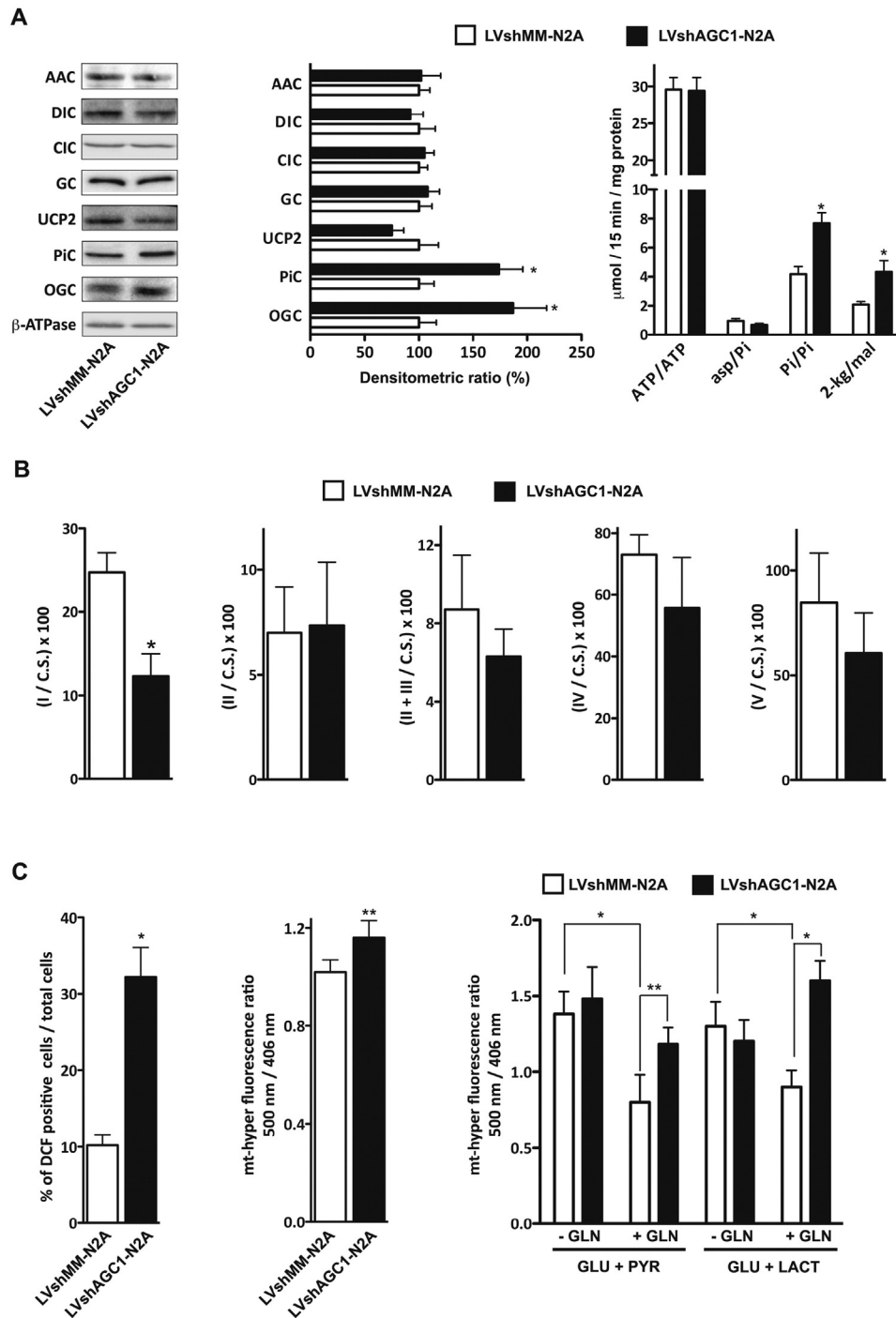
Fig. 6. Activities of mitochondrial carriers and respiratory chain complexes in N2A cells with down-regulated AGC1. (A) Mitochondrial carrier levels and activities in undifferentiated AGC1-silenced N2A cells. The expression of mitochondrial ADP/ATP carrier (AAC), dicarboxylate carrier (DIC), citrate carrier (CIC), glutamate carrier (GC), uncoupling protein 2 (UCP2), phosphate carrier (PiC), 2-oxoglutarate/malate carrier (OGC) and β-ATPase were determined by densitometric analysis on western blots performed on mitochondrial extracts from LVshMM-N2A (white bars) and LVshAGC1-N2A cells (black bars). The left panel shows representative images of three independent experiments performed with antibodies specific for the indicated proteins and relative intensity of protein bands are shown in the central panel (mean values $\pm$ SD, $n = 3$, $*p < 0.01$ compared to LVshMM-N2A mitochondria). The right panel shows the activities of the $[^{14}C]ATP_{ext}/ATP_{int}$, $[^{14}C]aspartate_{ext}/phosphate_{int}$, $[^{33}P]phosphate_{ext}/phosphate_{int}$ and $[^{14}C]2$-oxoglutarate$_{ext}$/malate$_{int}$ exchanges catalyzed by AAC, UCP2, PiC and OGC proteins, respectively, and assayed in liposomes reconstituted with the mitochondrial extracts of LVshMM-N2A or LVshAGC1-N2A cells. Transport was initiated by adding 0.1 mM of the indicated radiolabeled substrates to proteoliposomes preloaded with 20 mM of the indicated internal substrates. Data are means $\pm$ SD, $n = 3$, $*p < 0.01$ compared to liposomes reconstituted with LVshMM-N2A mitochondrial extracts, one-way analysis with Bonferroni t-test. (B) Mitochondrial respiratory chain complex activities in undifferentiated AGC1-silenced N2A cells. Activities of the indicated complexes in LVshMM-N2A (white bars) or LVshAGC1-N2A cells (black bars) were determined by spectrophotometry and related to citrate synthase (C.S.) activity which resulted unvaried in both cell types. Data are means $\pm$ SD, $n = 3$, $*p < 0.01$ compared to LVshMM-N2A cells, one-way analysis with Bonferroni t-test. (C) Cytosolic and mitochondrial hydrogen peroxide was measured in LVshMM-N2A (white bars) and LVshAGC1-N2A cells (black bars) loaded with 5 μM CM-H2DCFDA (left panel) or expressing the ratiometric H$_2$O$_2$-sensitive mt-HyPer protein (central and right panel). Measurements were performed in cells in complete rich DMEM (left and central panel) or incubated 1 h in MEM with 1 g/l glucose, 1 mM pyruvate or 5 mM lactate $\pm$ 2 mM glutamine. Data are means $\pm$ SD, $n = 3$, $*p < 0.01$, $**p < 0.05$ compared to LVshMM-N2A cells, one-way analysis with Bonferroni t-test.
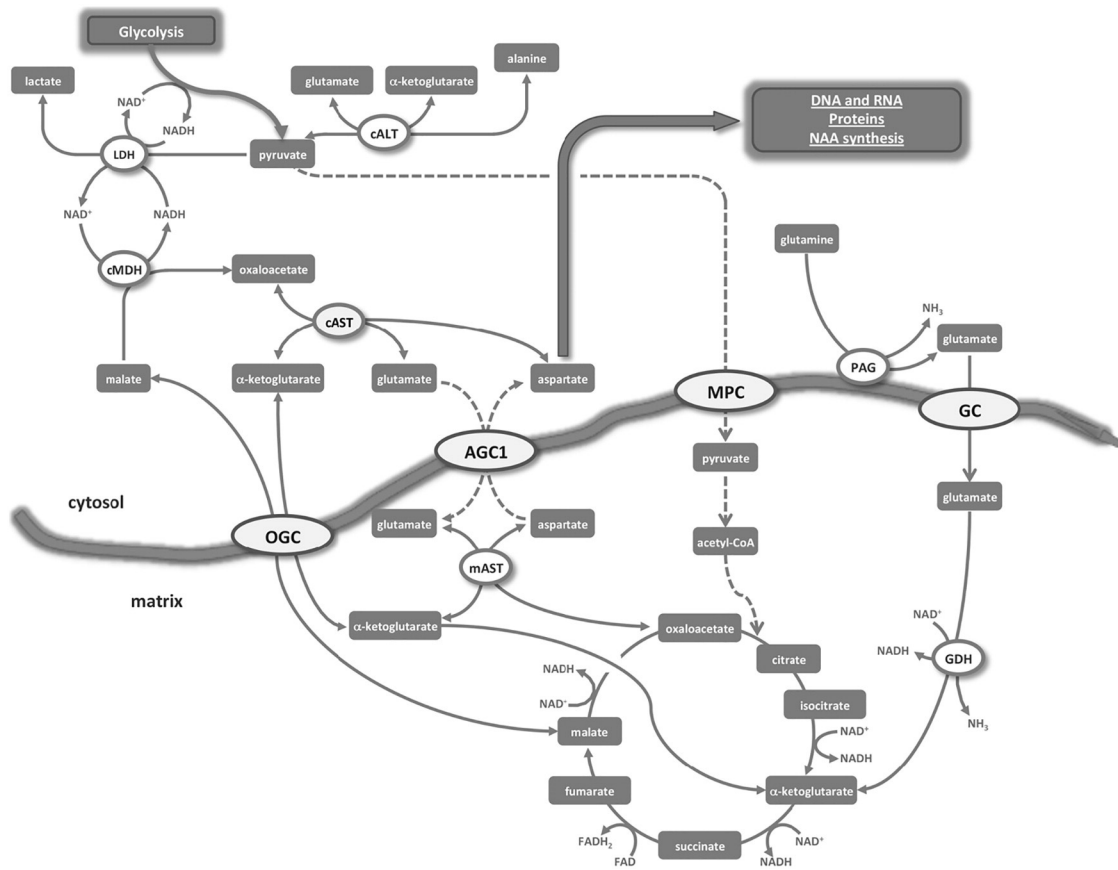
Fig. 7. Down-regulation of AGC1 in N2A cells impairs the malate/aspartate NADH shuttle and mitochondrial pyruvate oxidation. Glutamine oxidation generates energy by stimulating a partial TCA cycle and promotes an alternative pathway for the synthesis of aspartate which is indispensable for nucleic acid, protein and NAA synthesis. Dashed lines indicate inhibited pathways. In the present scheme, phosphate-activated glutaminase (PAG) is assumed to be localized on the external side of the inner mitochondrial membrane [71]. GDH, glutamic dehydrogenase; OGC, 2-oxoglutarate/malate carrier; MPC, pyruvate carrier; GC, glutamate carrier; LDH, lactic dehydrogenase; cMDH, cytosolic malic dehydrogenase; cAST and mAST, cytosolic and mitochondrial aspartic transaminase; ALT, alanine transaminase.

substrates, AGC1 impairment brings undifferentiated N2A cells to an energetic deficit (Fig. 3A and B) which may underlie the boosted apoptotic processes compromising normal cell viability (Fig. 2A and B) [59]. This is particularly true when lactate is used. The oxidation of this substrate
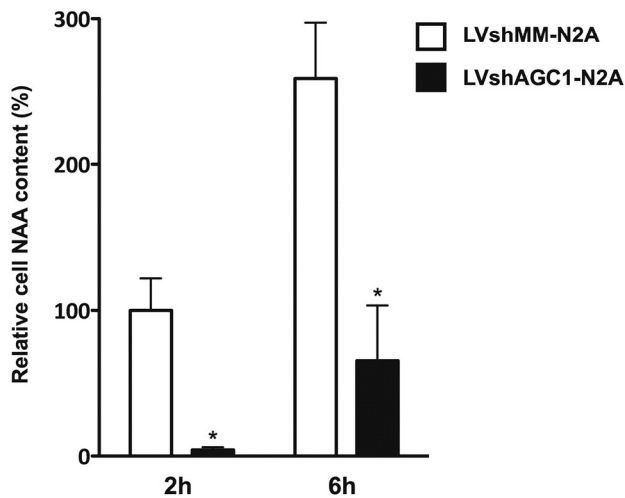
Fig. 8. Down-regulation of AGC1 reduces the content of N-acetylaspartate in N2A cells. Relative N-acetylaspartate concentrations were determined by mass spectrometry in LVshMM-N2A and LVshAGC1-N2A cells harvested after 1- or 6-h incubation with MEM supplemented with 1 g/l glucose, 5 mM lactate and 2 mM glutamine. Error bars represent the SD of four independent preparations; $*p < 0.01$ compared to LVshMM-N2A cells, one-way analysis with Bonferroni t-test.

generates in neurons an additional quota of cytosolic NADH [60] which cannot be correctly re-oxidized in mitochondria with impaired AGC1, thus further unbalancing the cellular redox state. Conversely, we observed that even in the absence of functional MAS, the addition of glutamine to the cellular medium apparently re-establishes a normal bioenergetic profile of N2A cells, as shown in terms of basal respiration, ATP turnover and mitochondrial respiration capacity, and restores cell survival. It has been documented that in hypoglycemic conditions neurons actively use glutamine and in turn glutamate as alternative fuels to sustain energy production by entering the TCA cycle at the level of 2-oxoglutarate dehydrogenase [61]. Accordingly, our data demonstrated that undifferentiated N2A cells with down-regulated AGC1 scarcely oxidize pyruvate, but have a higher disposition to take and consume glutamine (Fig. 5). As expected, glutamine consumption appears not to interfere with pyruvate oxidation, since higher lactate synthesis occurs in AGC1-silenced N2A cells either grown in rich medium with glutamine (Fig. 1D) or stimulated with the Ca^{2+}-releasing agonist ATP even in the presence of glutamine (see ECAR changes in Fig. 4A), i.e. when pyruvate oxidation is maximized [10]. According to our data, it could be suggested that in the brain with impaired AGC1 [4,5], neuronal progenitors could survive only if appropriate glutamine concentrations are available. It should be noted that astrocytes supply glutamine to neurons [62] by a process called glutamate-glutamine cycle where part of the neuronally released glutamate is converted by the astrocytic-specific enzyme glutamine synthase (GS) to glutamine which is then transferred back to neurons. Moreover, through aerobic glycolysis, astrocytes carry out net synthesis of glutamate and glutamine, as well as of TCA cycle intermediates and related derivatives whose traffic to neurons has been demonstrated [63]. To our knowledge, the consequences

of AGC1 impairment in astrocytes have not yet been evaluated exhaustively and negative effects on their intense oxidative metabolism, and in turn on neuron nourishment, cannot be excluded, thus further compromising the correct neuronal maturation process [16,64].

In neurons MAS is not only crucial for NADH transfer from cytosol to mitochondria, but also to allow the export of TCA cycle derivatives towards the cytosol via metabolite exchange processes [65,66 and refs. therein]. This is indispensable when biosynthetic processes occur and intermediates such as oxoglutarate, malate and oxaloacetate (OAA) are diverted away from the TCA cycle to supply the otherwise consumed amino and keto acid pools in the cytoplasm. In this context, anaplerotic reactions are essential. However, anaplerotic enzymes, such as pyruvate carboxylase and malic enzyme, would be of scarce utility without mitochondrial pyruvate oxidation, and appear to be abundant in astrocytes, while absent in neurons [66–68]. If this is the case also in proliferating undifferentiated neurons, exchange activity of the mitochondrial transporters involved in MAS would represent a potential preferential path to move intermediates required for biosynthesis. As a consequence, AGC1 impairment in N2A cells may result in unbalancing the integration of cytosolic keto and amino acid pools, in particular aspartate. Aspartate is essential for many cell processes since it participates in protein and nucleotide syntheses, and is the main metabolic product of respiration in proliferating cells, as recently reported [18,45]. Importantly, glutamine oxidation by neurons results in massive formation of aspartate [69,70]. Nevertheless, since the main site of aspartate production is the mitochondrial matrix [18], the absence of functional AGC1 in N2A cells proliferating with glutamine would make the inner mitochondrial membrane inaccessible for aspartate exit unless other transporters intervene. To our knowledge, the mitochondrial UCP2 is the only alternative candidate to transport aspartate out of mitochondria [20]. However, our data reveal that in mitochondria from AGC1-silenced N2A cells, aspartate transport catalyzed by UCP2 appears not to compensate the dramatic reduction of aspartate/glutamate exchange activity (compare Figs. 1C and 6A). Conversely, we show that N2A cells respond to AGC1 reduction with augmented expression and activity of both mitochondrial PIC and OGC. Increased PIC levels could be required to sustain mitochondrial ATP synthesis rates, as for example measured when cells were triggered with Ca^{2+}-releasing agonists (Fig. 4E). Overexpression of OGC could be interpreted on one side as a biochemical adaptation to sustain the weakened MAS activity. On the other side, in the presence of glutamine supply, increased OGC might diversely favor the exit of C4 metabolites from the TCA cycle, specifically malate (Fig. 7). In mitochondria, glutamine-derived glutamate [71,72] is converted to 2-oxoglutarate by both glutamic dehydrogenase (GDH) and aspartic transaminase (AST). 2-Oxoglutarate entering into a partial TCA cycle generates energy and furnishes OAA for the formation of aspartate by AST, as well [61]. In our hypothesis, in AGC1 deficient N2A cells, fueled 2-oxoglutarate oxidation favors increased OCR, but impeded efflux of mitochondrial aspartate may in turn inhibit the amination of exceeding OAA by mitochondrial AST. As a result, the augmented mass of C4 TCA intermediates following glutamine oxidation may generate additional mitochondrial malate which could be released in the cytosol by overexpressed OGC whose bidirectional transport activity is not constrained by the mitochondrial membrane potential [65]. In the cytosol, oxidation of malate by MDH may both produce further lactate and generate OAA which subsequently aminated by cytosolic AST would complete an alternative path for aspartate synthesis in the cytosol. However, the adaptation mechanism boosted by glutamine oxidation, although preserving cell proliferation, appears to lead AGC1 deficient cells to the metabolic sequela of higher oxidative stress (Fig. 6C), most likely due to the observed lower activity of respiratory complex I, a well-known site of ROS production [41] which may inaccurately handle the flux of NADH generated by glutamine oxidation. The reduced aspartate content revealed in proliferating AGC1-silenced cells (Fig. 5), could therefore be interpreted as a high utilization of this amino acid for protein and nucleotide synthesis purposes during cell growth and division

[18]. In addition, the required aspartate synthesis might likely be less efficient in AGC1-silenced cells than in normal cells, and therefore other aspartate-requiring cellular processes may be disadvantaged. This may explain the reduced NAA synthesis measured in AGC1 deficient N2A cells (Fig. 8). NAA is formed from aspartate and acetyl-CoA by the neuron-specific aspartate N-acetyltransferase (Asp-NAT). NAA is thought to be a molecule carrying acetyl groups for the formation of myelin lipids in oligodendrocytes. Reduced NAA content is observed in patients with AGC1 deficiency who suffer of hypomyelination and cerebral volume loss [4,5]. Indeed, in AGC1 deficient cells, NAA production might be compromised by the limited availability of both Asp-NAT reagents. Pyruvate oxidation is the main source of acetyl-CoA. In particular, when exceeding pyruvate oxidation occurs, the additional mitochondrial citrate produced in the TCA cycle is exported out in the cytosol and then cleaved by citrate lyase, thus providing acetyl-CoA for biosynthetic purposes. Therefore, it could be suggested that when AGC1 is inactivated, the subsequent MAS impairment impedes efficient pyruvate oxidation [10] and may prevent the formation of appropriate acetyl-CoA levels for NAA synthesis. In this case, ketone bodies or amino acids, such as leucine, bypassing the metabolic block caused by AGC1 deficit, would provide a direct source of acetyl-CoA [73] which in the presence of appropriate aspartate levels could rescue NAA synthesis. This hypothesis is consistent with the recently reported case of a patient affected by AGC1 deficiency who has been successfully treated with a ketogenic diet leading to clear improvement of psychomotor development and restored myelination [74]. However, we did not measure any significant change in citrate levels in AGC1 deficient N2Acells and further experiments are needed to clarify whether the normal levels of this metabolite coincide with sufficient supply of acetyl-CoA for NAA synthesis. In addition, our data do not allow discerning whether reduced pyruvate oxidation inhibits NAA synthesis in mitochondria or cytosol.

5. Conclusions

Together our results allow us to hypothesize a pivotal function of AGC1 in the needs of undifferentiated neurons, not only by maintaining a balanced energy metabolism through correct pyruvate oxidation, but also by warranting appropriate provision of crucial biosynthetic metabolites in the cytosol, in particular aspartate and acetyl-CoA. In view of further experimentation to be performed with human cell models, for instance with AGC1 activity comparable to that observed in AGC1-silenced N2A cells [5], our results demonstrate that loss of AGC1 is incompatible with undifferentiated neuron proliferation and NAA synthesis. Furthermore, compensatory pathways, such as increased glutaminolysis and alternative aspartate biosynthesis are most likely induced to allow the survival of dividing neurons, and their investigation may be crucial to clarify the metabolic changes occurring in developing brain with AGC1 deficiency.

Transparency document

The Transparency document associated with this article can be found, in online version.

References

[1] L. Palmieri, B. Pardo, F.M. Lasorsa, A. del Arco, K. Kobayashi, M. Iijima, M.J. Runswick, J.E. Walker, T. Saheki, J. Satrústegui, F. Palmieri, Citrin and aralar1 are Ca^{2+}-stimulated aspartate/glutamate transporters in mitochondria, EMBO J. 20 (2001) 5060–5069.

[2] F.M. Lasorsa, P. Pinton, L. Palmieri, G. Fiermonte, R. Rizzuto, F. Palmieri, Recombinant expression of the Ca²⁺-sensitive aspartate/glutamate carrier increases mitochondrial ATP production in agonist-stimulated Chinese hamster ovary cells, J. Biol. Chem. 278 (2003) 38686–38692.

[3] F. Palmieri, Mitochondrial transporters of the SLC25 family and associated diseases: a review, J. Inherit. Metab. Dis. 37 (2014) 565–575.

[4] R. Wibom, F.M. Lasorsa, V. Töhönen, M. Barbaro, F.H. Sterky, T. Kucinski, K. Naess, M. Jonsson, C.L. Pierri, F. Palmieri, A. Wedell, AGC1 deficiency associated with global cerebral hypomyelination, N. Engl. J. Med. 361 (2009) 489–495.

[5] M.J. Falk, D. Li, X. Gai, E. McCormick, E. Place, F.M. Lasorsa, F.G. Otieno, C. Hou, C.E. Kim, N. Abdel-Magid, L. Vazquez, F.D. Mentch, R. Chiavacci, J. Liang, X. Liu, H. Jiang, G. Giannuzzi, E.D. Marsh, G. Yiran, L. Tian, F. Palmieri, H. Hakonarson, AGC1 deficiency causes infantile epilepsy, abnormal myelination, and reduced N-acetylaspartate, JIMD Reports, Springer Science + Business Media 2014, pp. 77–85.

[6] K. Kobayashi, D.S. Sinasac, M. Iijima, A.P. Boright, L. Begum, J.R. Lee, T. Yasuda, S. Ikeda, R. Hirano, H. Terazono, M.A. Crackower, I. Kondo, L.C. Tsui, S.W. Scherer, T. Saheki, The gene mutated in adult-onset type II citrullinaemia encodes a putative mitochondrial carrier protein, Nat. Genet. 22 (1999) 159–163.

[7] M. Iijima, A. Jalil, L. Begum, T. Yasuda, N. Yamaguchi, M. Xian Li, N. Kawada, H. Endou, K. Kobayashi, T. Saheki, Pathogenesis of adult-onset type II citrullinemia caused by deficiency of citrin, a mitochondrial solute carrier protein: tissue and subcellular localization of citrin, Adv. Enzym. Regul. 41 (2001) 325–342.

[8] T. Saheki, K. Kobayashi, Mitochondrial aspartate glutamate carrier (citrin) deficiency as the cause of adult-onset type II citrullinemia (CTLN2) and idiopathic neonatal hepatitis (NICCD), J. Hum. Genet. 47 (2002) 333–341.

[9] Z.-H. Lu, G. Chakraborty, R.W. Ledeen, D. Yahya, G. Wu, N-Acetylaspartate synthase is bimodally expressed in microsomes and mitochondria of brain, Mol. Brain Res. 122 (2004) 71–78.

[10] I. Llorente-Folch, C.B. Rueda, I. Amigo, A. del Arco, T. Saheki, B. Pardo, J. Satrustegui, Calcium-regulation of mitochondrial respiration maintains ATP homeostasis and requires ARALAR/AGC1-malate aspartate shuttle in intact cortical neurons, J. Neurosci. 33 (2013) 13957–13971.

[11] A. Menga, V. Iacobazzi, V. Infantino, M.L. Avantaggiati, F. Palmieri, The mitochondrial aspartate/glutamate carrier isoform 1 gene expression is regulated by CREB in neuronal cells, Int. J. Biochem. Cell Biol. 60 (2015) 157–166.

[12] L. Contreras, A. Urbieta, K. Kobayashi, T. Saheki, J. Satrustegui, Low levels of citrin (SLC25A13) expression in adult mouse brain restricted to neuronal clusters, J. Neurosci. Res. 88 (2010) 1009–1016.

[13] M. Ramos, A. del Arco, B. Pardo, A. Martínez-Serrano, J.R. Martínez-Morales, K. Kobayashi, T. Yasuda, E. Bógónez, P. Bovolenta, T. Saheki, J. Satrústegui, Developmental changes in the Ca²⁺-regulated mitochondrial aspartate–glutamate carrier aralar1 in brain and prominent expression in the spinal cord, Dev. Brain Res. 143 (2003) 33–46.

[14] D. Lovatt, U. Sonnewald, H.S. Waagepetersen, A. Schousboe, W. He, J.H.C. Lin, X. Han, T. Takano, S. Wang, F.J. Sim, S.A. Goldman, M. Nedergaard, The transcriptome and metabolic gene signature of protoplasmic astrocytes in the adult murine cortex, J. Neurosci. 27 (2007) 12255–12266.

[15] B. Pardo, T.B. Rodrigues, L. Contreras, M. Garzón, I. Llorente-Folch, K. Kobayashi, T. Saheki, S. Cerdan, J. Satrústegui, Brain glutamine synthesis requires neuronal-born aspartate as amino donor for glial glutamate formation, J. Cereb. Blood Flow Metab. 31 (2011) 90–101.

[16] B. Li, L. Hertz, L. Peng, Aralar mRNA and protein levels in neurons and astrocytes freshly isolated from young and adult mouse brain and in maturing cultured astrocytes, Neurochem. Int. 61 (2012) 1325–1332.

[17] T. Sakurai, N. Ramoz, M. Barreto, M. Gazdoiu, N. Takahashi, M. Gertner, N. Dorr, M.A. Gama Sosa, R. De Gasperi, G. Perez, J. Schmeidler, V. Mitropoulou, H.C. Le, M. Lupu, P.R. Hof, G.A. Elder, J.D. Buxbaum, Slc25a12 disruption alters myelination and neurofilaments: a model for a hypomyelination syndrome and childhood neurodevelopmental disorders, Biol. Psychiatry 67 (2010) 887–894.

[18] Lucas B. Sullivan, Dan Y. Gui, Aaron M. Hosios, Lauren N. Bush, E. Freinkman, Matthew G. Vander Heiden, Supporting aspartate biosynthesis is an essential function of respiration in proliferating cells, Cell 162 (2015) 552–563.

[19] B. Yuan, R. Latek, M. Hossbach, T. Tuschl, F. Lewitter, siRNA selection server: an automated siRNA oligonucleotide prediction server, Nucleic Acids Res. 32 (2004) W130–W134.

[20] A. Vozza, G. Parisi, F. De Leonardis, F.M. Lasorsa, A. Castegna, D. Amorese, R. Marmo, V.M. Calcagnile, L. Palmieri, D. Ricquier, E. Paradies, P. Scarcia, F. Palmieri, F. Bouillaud, G. Fiermonte, UCP2 transports C4 metabolites out of mitochondria, regulating glucose and glutamine oxidation, Proc. Natl. Acad. Sci. U. S. A. 111 (2014) 960–965.

[21] M. Casimir, F.M. Lasorsa, B. Rubi, D. Caille, F. Palmieri, P. Meda, P. Maechler, Mitochondrial glutamate carrier GC1 as a newly identified player in the control of glucose-stimulated insulin secretion, J. Biol. Chem. 284 (2009) 25004–25014.

[22] C. Indiveri, K. Kramer, F. Palmieri, Reconstitution of the malate/aspartate shuttle from mitochondria, J. Biol. Chem. 262 (1987) 15979–15983.

[23] Martin D. Brand, David G. Nicholls, Assessing mitochondrial dysfunction in cells, Biochem. J. 435 (2011) 297–312.

[24] E. Gnaiger, Polarographic oxygen sensors, the oxygraph, and high-resolution respirometry to assess mitochondrial function, Drug-induced Mitochondrial Dysfunction, Wiley-Blackwell 2008, pp. 325–352.

[25] S.W. Choi, A.A. Gerencser, R. Ng, J.M. Flynn, S. Melov, S.R. Danielson, B.W. Gibson, D.G. Nicholls, D.E. Bredesen, M.D. Brand, No consistent bioenergetic defects in presynaptic nerve terminals isolated from mouse models of Alzheimer's disease, J. Neurosci. 32 (2012) 16775–16784.

[26] M. Bonora, C. Giorgi, A. Bononi, S. Marchi, S. Patergnani, A. Rimessi, R. Rizzuto, P. Pinton, Subcellular calcium measurements in mammalian cells using jellyfish photoprotein aequorin-based probes, Nat. Protoc. 8 (2013) 2105–2118.

[27] V.V. Belousov, A.F. Fradkov, K.A. Lukyanov, D.B. Staroverov, K.S. Shakhbazov, A.V. Terskikh, S. Lukyanov, Genetically encoded fluorescent indicator for intracellular hydrogen peroxide, Nat. Methods 3 (2006) 281–286.

[28] J.M. Suski, M. Lebiedzinska, M. Bonora, P. Pinton, J. Duszynski, M.R. Wieckowski, Relation between mitochondrial membrane potential and ROS formation, Mitochondrial Bioenergetics, Springer Science + Business Media 2011, pp. 183–205.

[29] F.N. Gellerich, J.A. Mayr, S. Reuter, W. Sperl, S. Zierz, The problem of interlab variation in methods for mitochondrial disease diagnosis: enzymatic measurement of respiratory chain complexes☆, Mitochondrion 4 (2004) 427–439.

[30] P.-Y. Wu, Y.-C. Lin, C.-L. Chang, H.-T. Lu, C.-H. Chin, T.-T. Hsu, D. Chu, S.H. Sun, Functional decreases in P2X7 receptors are associated with retinoic acid-induced neuronal differentiation of Neuro-2a neuroblastoma cells, Cell. Signal. 21 (2009) 881–891.

[31] A. Ma'ayan, S.L. Jenkins, A. Barash, R. Iyengar, Neuro2A differentiation by G i/o pathway, Sci. Signal. 2 (2009) (cm1-cm1).

[32] U.V. Wesley, J.F. Hatcher, R.J. Dempsey, Sphingomyelin synthase 1 regulates neuro-2a cell proliferation and cell cycle progression through modulation of p27 expression and Akt signaling, Mol. Neurobiol. 51 (2015) 1530–1541.

[33] G. Fiermonte, L. Palmieri, S. Todisco, G. Agrimi, F. Palmieri, J.E. Walker, Identification of the mitochondrial glutamate transporter - Bacterial expression, reconstitution, functional characterization, and tissue distribution of two human isoforms, J. Biol. Chem. 277 (2002) 19289–19294.

[34] J.M. Pascual, F. Carceller, J.M. Roda, S. Cerdan, R.C. Koehler, Glutamate, glutamine, and GABA as substrates for the neuronal and glial compartments after focal cerebral ischemia in rats editorial comment, Stroke 29 (1998) 1048–1057.

[35] A.G. Porter, R.U. Jänicke, Emerging roles of caspase-3 in apoptosis, Cell Death Differ. 6 (1999) 99–104.

[36] C. Soldani, M.C. Lazzè, M.G. Bottone, G. Tognon, M. Biggiogera, C.E. Pellicciari, A.I. Scovassi, Poly(ADP-ribose) polymerase cleavage during apoptosis: when and where? Exp. Cell Res. 269 (2001) 193–201.

[37] P. Pinton, C. Giorgi, R. Siviero, E. Zecchini, R. Rizzuto, Calcium and apoptosis: ER-mitochondria Ca²⁺ transfer in the control of apoptosis, Oncogene 27 (2008) 6407–6418.

[38] K.S. McCommis, Z. Chen, X. Fu, W.G. McDonald, J.R. Colca, R.F. Kletzien, S.C. Burgess, B.N. Finck, Loss of mitochondrial pyruvate carrier 2 in the liver leads to defects in gluconeogenesis and compensation via pyruvate-alanine cycling, Cell Metab. 22 (2015) 682–694.

[39] I. Nissim, Newer aspects of glutamine/glutamate metabolism: the role of acute pH changes, Am. J. Phys. 277 (1999) F493–F497.

[40] F. Palmieri, M. Monné, Discoveries, metabolic roles and diseases of mitochondrial carriers: a review, Biochim. Biophys. Acta Mol. Cell Res. 1863 (2016) 2362–2378.

[41] J. Hirst, Martin S. King, Kenneth R. Pryde, The production of reactive oxygen species by complex I, Biochem. Soc. Trans. 36 (2008) 976–980.

[42] S. Verkaart, W.J.H. Koopman, S.E. van Emst-de Vries, L.G.J. Nijtmans, L.W.P.J. van den Heuvel, J.A.M. Smeitink, P.H.G.M. Willems, Superoxide production is inversely related to complex I activity in inherited complex I deficiency, Biochim. Biophys. Acta (BBA) - Mol. Basis Dis. 1772 (2007) 373–381.

[43] L. Flinn, H. Mortiboys, K. Volkmann, R.W. Koster, P.W. Ingham, O. Bandmann, Complex I deficiency and dopaminergic neuronal cell loss in parkin-deficient zebrafish (Danio rerio), Brain 132 (2009) 1613–1623.

[44] D. Ramonet, C. Perier, A. Recasens, B. Dehay, J. Bové, V. Costa, L. Scorrano, M. Vila, Optic atrophy 1 mediates mitochondria remodeling and dopaminergic neurodegeneration linked to complex I deficiency, Cell Death Differ. 20 (2012) 77–85.

[45] K. Birsoy, T. Wang, W.W. Chen, E. Freinkman, M. Abu-Remaileh, D.M. Sabatini, An essential role of the mitochondrial electron transport chain in cell proliferation is to enable aspartate synthesis, Cell 162 (2015) 540–551.

[46] C.N. Madhavarao, C. Chinopoulos, K. Chandrasekaran, M.A.A. Namboodiri, Characterization of the N-acetylaspartate biosynthetic enzyme from rat brain, J. Neurochem. 86 (2003) 824–835.

[47] G. Tahay, E. Wiame, D. Tyteca, Pierre J. Courtoy, E. Van Schaftingen, Determinants of the enzymatic activity and the subcellular localization of aspartate N-acetyltransferase, Biochem. J. 441 (2012) 105–112.

[48] M. Agostini, F. Romeo, S. Inoue, M.V. Niklison-Chirou, A.J. Elia, D. Dinsdale, N. Morone, R.A. Knight, T.W. Mak, G. Melino, Metabolic reprogramming during neuronal differentiation, Cell Death Differ. 23 (2016) 1502–1514.

[49] B. Mlody, C. Lorenz, G. Inak, A. Prigione, Energy metabolism in neuronal/glial induction and in iPSC models of brain disorders, Semin. Cell Dev. Biol. 52 (2016) 102–109.

[50] W.J. Koopman, P.H. Willems, J.A. Smeitink, Monogenic mitochondrial disorders, N. Engl. J. Med. 366 (2012) 1132–1141.

[51] C. Viscomi, E. Bottani, M. Zeviani, Emerging concepts in the therapy of mitochondrial disease, Biochim. Biophys. Acta Bioenerg. 1847 (2015) 544–557.

[52] V.A. Rafalski, A. Brunet, Energy metabolism in adult neural stem cell fate, Prog. Neurobiol. 93 (2011) 182–203.

[53] P. Mergenthaler, U. Lindauer, G.A. Dienel, A. Meisel, Sugar for the brain: the role of glucose in physiological and pathological brain function, Trends Neurosci. 36 (2013) 587–597.

[54] L. Hertz, The astrocyte-neuron lactate shuttle: a challenge of a challenge, J. Cereb. Blood Flow Metab. (2004) 1241–1248.

[55] A.B. Patel, J.C.K. Lai, G.M.I. Chowdhury, F. Hyder, D.L. Rothman, R.G. Shulman, K.L. Behar, Direct evidence for activity-dependent glucose phosphorylation in neurons with implications for the astrocyte-to-neuron lactate shuttle, Proc. Natl. Acad. Sci. 111 (2014) 5385–5390.

[56] P. Mächler, Matthias T. Wyss, M. Elsayed, J. Stobart, R. Gutierrez, A. von Faber-Castell, V. Kaelin, M. Zuend, A. San Martín, I. Romero-Gómez, F. Baeza-Lehnert, S. Lengacher, Bernard L. Schneider, P. Aebischer, Pierre J. Magistretti, L.F. Barros, B. Weber, In vivo evidence for a lactate gradient from astrocytes to neurons, Cell Metab. 23 (2016) 94–102.

[57] N.H.T. Nguyen, A. Bråthe, B. Hassel, Neuronal uptake and metabolism of glycerol and the neuronal expression of mitochondrial glycerol-3-phosphate dehydrogenase, J. Neurochem. 85 (2003) 831–842.

[58] Siesjo, Brain energy metabolism by B.K. Siesjo, John Wiley & Sons, New York, 1978, Ann. Neurol. 5 (1979).

[59] M.L. Boland, A.H. Chourasia, K.F. Macleod, Mitochondrial dysfunction in cancer, Front. Oncol. 3 (2013).

[60] J.M. Petit, P.J. Magistretti, Regulation of neuron–astrocyte metabolic coupling across the sleep–wake cycle, Neuroscience 323 (2016) 135–156.

[61] M. Erecińska, M.M. Zaleska, D. Nelson, I. Nissim, M. Yudkoff, Neuronal glutamine utilization: glutamine/glutamate homeostasis in synaptosomes, J. Neurochem. 54 (1990) 2057–2069.

[62] L. Hertz, L. Peng, G.A. Dienel, Energy metabolism in astrocytes: high rate of oxidative metabolism and spatiotemporal dependence on glycolysis/glycogenolysis, J. Cereb. Blood Flow Metab. 27 (2007) 219–249.

[63] L. Hertz, L. Peng, G.A. Dienel, Energy metabolism in astrocytes: high rate of oxidative metabolism and spatiotemporal dependence on glycolysis/glycogenolysis, J. Cereb. Blood Flow Metab. 27 (2006) 219–249.

[64] L. Hertz, Brain glutamine synthesis requires neuronal aspartate: a commentary, J. Cereb. Blood Flow Metab. 31 (2011) 384–387.

[65] F. Palmieri, The mitochondrial transporter family SLC25: identification, properties and physiopathology, Mol. Asp. Med. 34 (2013) 465–484.

[66] L. Hertz, G.A. Dienel, Energy metabolism in the brain, International Review of Neurobiology, Elsevier BV 2002, pp. 1–IN4.

[67] A.C.H. Yu, J. Drejer, L. Hertz, A. Schousboe, Pyruvate carboxylase activity in primary cultures of astrocytes and neurons, J. Neurochem. 41 (1983) 1484–1487.

[68] G.M. Kurz, H. Wiesinger, B. Hamprecht, Purification of cytosolic malic enzyme from bovine brain, generation of monoclonal antibodies, and immunocytochemical localization of the enzyme in glial cells of neural primary cultures, J. Neurochem. 60 (1993) 1467–1474.

[69] M.C. McKenna, The glutamate-glutamine cycle is not stoichiometric: fates of glutamate in brain, J. Neurosci. Res. 85 (2007) 3347–3358.

[70] R.W. Briggs, Review of "magnetic resonance spectroscopy and imaging in neurochemistry" (edited by Herman Bachelard), volume 8 of advances in neurochemistry (series editors: B.W. Agranoff and K. Suzuki) for spectroscopy letters, Spectrosc. Lett. 31 (1998) 1123–1124.

[71] E. Kvamme, I.A. Torgner, B.r. Roberg, Kinetics and localization of brain phosphate activated glutaminase, J. Neurosci. Res. 66 (2001) 951–958.

[72] A. Cassago, A.P. Ferreira, I.M. Ferreira, C. Fornezari, E.R. Gomes, K.S. Greene, H.M. Pereira, R.C. Garratt, S.M. Dias, A.L. Ambrosio, Mitochondrial localization and structure-based phosphate activation mechanism of glutaminase C with implications for cancer metabolism, Proc. Natl. Acad. Sci. U. S. A. 109 (2012) 1092–1097.

[73] B. Vanderperre, S. Herzig, P. Krznar, M. Hörl, Z. Ammar, S. Montessuit, S. Pierredon, N. Zamboni, J.-C. Martinou, Embryonic lethality of mitochondrial pyruvate carrier 1 deficient mouse can be rescued by a ketogenic diet, PLoS Genet. 12 (2016), e1006056. .

[74] M. Dahlin, D.A. Martin, Z. Hedlund, M. Jonsson, U. von Döbeln, A. Wedell, The ketogenic diet compensates for AGC1 deficiency and improves myelination, Epilepsia 56 (2015) e176–e181.